Dynamic Analysis of aMultilayered Poroviscoelastic ground Under aMoving Harmonic Load

K. CHAHOUR[a], G. LEFEUVE-MESGOUEZ[b], A. MESGOUEZ[b], B. SAFI[c]

a. Department of Civil Engineering, University MouloudMammeri of TiziOuzou RP. 15000, Algeria.
b.Department of Physics, Université d'Avignon et des Pays de Vaucluse. 33, rue Louis Pasteur, Avignon 84000, France.
c. Department of Materials Engineering, Faculty of Sciences, University M'hamedBougaraBoumerdes, Algeria.

Abstract:

This work deals about coupling a railway track with a multilayered poroviscoelastic soil medium. A moving harmonic rectangular excitation is applied either directly over the surface of the ground or over a track model. A semi-analytical approach based on the matrix method of the porous medium is proposed to resolve the dynamic problem. To get the influence of the railway track on soil dynamic response, a comparison between results given when the track is taken into account and the case where load is directly applied on the soil is also proposed. The amplitude of displacement response is given for various values of load velocity. Results are given in both the spatial and wavenumber domains.

Keywords:

Wave propagation, moving load, railway track, multilayered soil, wavenumber results, semi-analytical approach, Fourier transform.

1.Introduction

In the frame of moving train loads, many authors have worked to model the ground and the railway track. The three-dimensional half space subjected to a point load moving with a constant velocity was first, considered by Eason et al. [1]. Jones et al. [2] studied the case of a moving rectangular load overlying an elastic half-space. De Barros and Luco [3] investigated the response of a stratified viscoelastic half-space to a moving point load. Both these latter works demonstrate the possibility of shock formation in the ground. The ground is considered as viscoelastic media. However, Theodorakopoulos [4] showed that in the case of soft materials, models ignoring the coupling between fluid and solid may lead to errors, especially for high velocities. Using Biot'stheory, Cai et al. [5] presented a semi-analytical approach for a moving rectangular load of constant amplitude on a porous half-space. A comparison between viscoelastic and poroviscoelastic models shows that for higher load speeds, the poroviscoelastic soil displacements are larger than that of the viscoelastic soil whereas they are similar for low load speeds.Based on the concept of the equivalent stiffness of the half-space, Li Shi and Selvadurai [6] investigated the steady-state displacements and moments in an infinite Bernoulli–Euler beam resting on a poroelastic half-space subjected to a concentrated moving load**.** The authors gave expressions for the equivalent stiffness of the saturated medium interacting with the

infinite beam using a contour integration procedure. Comparisons have been made between situations for the elastic and poroelastic half-space with regard to their equivalent stiffness and the dynamic responses of the beam for different load velocities.

The Euler beam model is one of the most used models for representing the railway track.Based on an Euler beam evenly supported by a series of springs,Wang et al.[7] model the rail-sleeper-ballast system. The approach used is based on frequency shift to identify the damaged supports including the loose or missing fasteners and damaged ballast. The stiffness of which are reduced when the fastener is loose or missing and the ballast under the sleepers is damaged. An auxiliary mass is utilized herein and when it is mounted on the beam. The authors concluded the natural frequencies change periodically when the supports are undamaged, whereas the periodicity is broken due to damaged supports. A special damage index only using the information of the damaged states is proposed by the authors and both numerical and experimental examples are carried out to validate the proposed method.Xu et al. [8] show that for an Euler beam overlying a layered poroelastic half-space, there still exist critical velocities even when the load speed is larger than the shear wavespeed. Lefeuve-Mesgouez et al. [9] showed differences in the amplitude and distribution of solid displacements and fluid pressure of a poroviscoelasticlayered half-space when the track is taken into account.Sheng et al. [10] proposed a track model taking into account all the track components. This model is a reference for numerous works, Takemiya et al. [11], Picoux et al. [12], Cai et al.[13]. Moreover, studies concerning a more realistic track system implemented to porous stratified medium are rather limited.

In this paper, a semi-analytical approach is used to investigate the vertical dynamic response of a poroviscoelasticlayered ground. The soil is coupled to a Sheng's track model subjected to a vertical moving load. The implementation of the beam over the ground allows getting the effect of the track on the dynamic soil response. The case of a layer resting on a half-space is given in this paper. Thus, soil vertical displacements are numerically evaluated for various values of load speed, in both the wavenumber domain and the spatial domain.

2. Model Description

2.1. Geometry

The studied geometry is presented on Figure 10. The track model is based on Sheng's model overlying a layer resting on a rigid half-space. The railway is infinite in length and is aligned with respect to the x direction. The contact width with the ground is denoted $2L_{Bal}$.

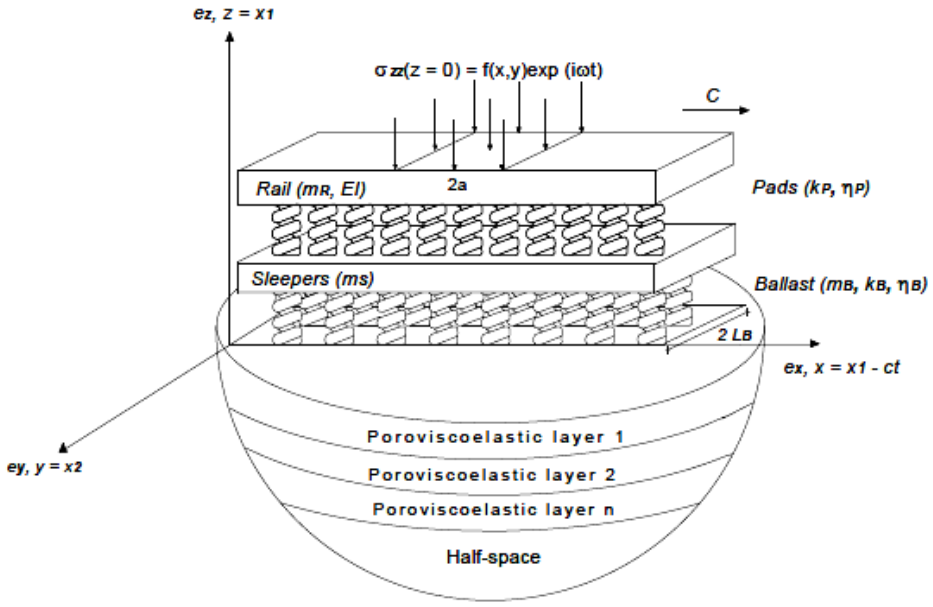

Figure 1: Railway track model.

2.2. Governing equations of the porous medium

In the proposed approach, speed waves, solid and fluid displacements are calculated analytically, for each soil point medium in both spatial and wavenumber domains. Based on the constitutive equations and the conservation of momentum, we obtain for each homogeneous and isotropic layer in the poroviscoelastic medium.

$$\begin{cases} \sigma = (\lambda_0 \nabla.\mathbf{u} - \beta p)\,\mathbf{I} + 2\mu\,\varepsilon, \\ p = -m\,(\beta \nabla.\mathbf{u} + \nabla.\mathbf{w}), \\ \nabla\sigma = \rho\,\ddot{\mathbf{u}} + \rho_f\,\ddot{\mathbf{w}}, \\ -\nabla p = \rho_f\,\ddot{\mathbf{u}} + \dfrac{a_\infty \rho_f}{\phi}\,\ddot{\mathbf{w}} + \dfrac{\eta}{\kappa}\,\dot{\mathbf{w}}, \end{cases} \tag{1}$$

Where $u = \langle u_{x1}, u_{x1}, u\rangle^t$ is the solid displacement vector, $U = \langle U_{x1}, U_{x1}, U_{x3}\rangle^t$ is thefluid displacement vector and $w = \phi(U-u) = \langle w_{x1}, w_{x1}, w_{x3}\rangle^t$, the relative displacement vector. I is the identity tensor, σ is the stress tensor, $\varepsilon = 1/2(\nabla u + \nabla^t \mathrm{u})$ is the linearized strain tensor, and p is the pore pressure. The physical parameters are: the dynamic viscosity η and the density ρ_f of the saturating fluid, the density $\rho_f$and the shear modulus μ of the elastic skeleton, the connected porosity ϕ, the tortuosity a_∞, the absolute permeability κ, the Lamé coefficient of the dry matrix λ_0, and the two Biotcoefficientsβ and m of the isotropic matrix. The dots and double dots denote respectively first and second time derivatives.

2.3. Track equations

The model used for the track was first presented by Sheng et al. [10] and is composed of the rail, the sleepers and the ballast. First, the rail is modeled as an infinite Euler viscoelastic beam, for which the cross-section is supposed to be infinitely rigid, as follows

$$EIw_R(x_1,t)_{,x_1x_1x_1x_1} + m_R\ddot{w}_R(x_1,t) + k_P[w_R(x_1,t) - w_S(x_1,t)] = Q(x_1,t) \quad (2)$$

Where w_R and $w_S$are the deflections (i.e. vertical displacements) of the rail and the sleeper respectively, *EI* the bending rigidity of the rail, m_R the mass per unit of length of the rail.*kP* represents the spring constant per unit of length of the pads between the rail and the sleeper. *Q* is the applied moving load. For a load distributed over a non-zero width,$Q(x_1,t) = \frac{Q_0 \exp(i\omega t)}{2a} if: |x| = |x_1 - 1| < a$. The sleepers can be modeled using the concept of continuous mass: vertical displacements generated by a moving load are almost identical when taking into account a discrete or uniformly distributed distribution of sleepers, see Vostroukhov et al. [14]. The rail pads are modeled as a distributed vertical spring between the rail beam and the sleeper mass. Consequently, for the sleepers, the model is written as follows

$$m_S\ddot{w}_S(x_1,t) + k_P[w_S(x_1,t) - w_R(x_1,t)] = F_S(x_1,t) \quad (3)$$

Where FS stands for the sleeper vertical force per unit of length acting on the ballast, and mS the mass per unit of length of the sleeper. The ballast is modeled as a poroviscoelastic layer with uniformlydistributed mass. At the top and the bottom of the ballast, from Suiker et al. [15], the following equations are written

$$m_B/6[2\ddot{w}_S(x_1,t) + \ddot{w}_B(x_1,t)] + k_B[w_S(x_1,t) - w_B(x_1,t)] = -F_S(x_1,t) \quad (4)$$
$$m_B/6[\ddot{w}_S(x_1,t) + 2\ddot{w}_B(x_1,t)] + k_B[-w_S(x_1,t) + w_B(x_1,t)] = F_B(x_1,t) \quad (5)$$

Where F_B represents the vertical force per unit of length exerted by the ballast on the soil and w_B thevertical displacement of the ballast. k_B and m_B are the spring constant per unit of length and the mass per unit of length of the ballast. Dampings in pads and ballast are taken into account using a modified hysteretic damping with constants $\eta_P$and η_B.

2.4. Interface conditions

The interface conditions between the ballast and the ground, for $x_3 = 0$, are written as follows

$$\sigma_{33}(x_1,x_2,x_3=0) = \frac{-F_B}{2L_{Bal}} if\ |x_2| < L_{Bal} \quad (6)$$
$$\sigma_{13}(x_1,x_2,x_3=0) = 0 \quad \sigma_{23}(x_1,x_2,x_3=0) = 0 \quad (7)$$
$$p(x_1,x_2,x_3=0) = 0 \quad (8)$$
$$u_3(x_1,x_2,x_3=0) = w_B(x_1) \quad (9)$$

3. Matrix approach

The exact stiffness matrix approach is based on vectors of transformed displacement and stress components, see [16], defined as$\bar{\bar{u}}^* = \langle \bar{\bar{u}}_x^*, \bar{\bar{u}}_y^*, i\bar{\bar{u}}_z^*, i\bar{\bar{w}}_z^* \rangle^t$ and $\bar{\bar{\Sigma}}^* = \langle \bar{\bar{\sigma}}_{zz}^*, \bar{\bar{\sigma}}_{yz}^*, i\bar{\bar{\sigma}}_{zz}^*, , -i\bar{\bar{p}}^* \rangle^t$.Analytical expression for the vector of transformed displacements is then given by the solution of the matrix system

$$\underbrace{\begin{bmatrix} S^T & S^R z(h_n) \\ -S^T z(h_n) & -S^R \end{bmatrix}\begin{bmatrix} Q^T & Q^R z(h_n) \\ Q^T z(h_n) & Q^R \end{bmatrix}^{-1}}_{T^n_{(8\times 8)}} \begin{Bmatrix} \bar{\bar{u}}^*(z=z_{n-1}) \\ \bar{\bar{u}}^*(z=z_n \end{Bmatrix} = \begin{Bmatrix} \bar{\bar{\Sigma}}^*(z=z_{n-1}) \\ -\bar{\bar{\Sigma}}^*(z=z_n \end{Bmatrix} \quad (10)$$

Where $Q^{T/R}$, $S^{T/R}$ and Z(hn) are 4×4 matrices, h_n denotes the nth layer's depth. The superscripts *T*and *R* stand for transmitted and reflected waves, respectively. In the resulting vector $\bar{\bar{\Sigma}}^*$ all terms equal zero, except $\bar{\bar{\sigma}}_{zz}$ $(z=0)$ that is linked to the track using the interface conditions.

Considering the track equations (2, 3, 4 and 5), they are modified firstly by the change of variables, secondly by the Fourier transform on the *x* space variable, and thirdly by the elimination of$\bar{F}_s^*$ (k_x,ω). Consequently, the rail-sleeper-ballast system behavior is governed by 3 equations as follows

$$A_1(k_x,\omega)\overline{w_R}^*(k_x,\omega) - k_p\overline{w_S}^*(k_x,\omega) = A_2(k_x) \quad (11)$$

$$k_p\overline{w_R}^*(k_x,\omega) + A_3(k_x,\omega)\overline{w_S}^*(k_x,\omega) + A_4(k_x,\omega)\overline{w_B}^*(k_x,\omega) = 0 \quad (12)$$

$$A_4(k_x,\omega)\overline{w_S}^*(k_x,\omega) + A_5(k_x,\omega)\overline{w_B}^*(k_x,\omega) = -\overline{F_B}^*(k_x,\omega) \quad (13)$$

With

$A_1(k_x,\omega) = EIk_x^4 - m_R(\omega - k_x c)^2 + k_P$

$A_2(k_x,\omega) = \bar{Q}^*(k_x)$

$A_3(k_x,\omega) = m_S(\omega - k_x c)^2 + m_B/3(\omega - k_x c)^2 - k_P - k_B$

$A_4(k_x,\omega) = m_B/6(\omega - k_x c)^2 + k_B$

$A_5(k_x,\omega) = m_B/3(\omega - k_x c)^2 - k_B$

Where $\bar{Q}^*(k_x) = -Q_0\frac{\sin(ak_x)}{ak_x}$ for a load distributed over a non-zero width. $\bar{F}_B^*$is obtained with the interface condition between the ballast and the ground (6)

$$\overline{\overline{\sigma_{zz}}}_{|z=0}\left(k_x,k_y,\omega\right)^* = -\overline{F_B}^*(k_x,\omega)\frac{\sin(k_x L_{Bal})}{k_x L_{Bal}} \quad (14)$$

Thus we get four unknowns ($\overline{w}_R^*, \overline{w}_S^*, \overline{w}_B^*$and $\bar{F}_B^*$) for four equations (11, 12, 13, 14). From this system, it is of interest to get the expression for $\bar{F}_B^*$ as follows

$$\overline{F_B}^*(k_x,\omega) = \frac{-k_p A_2 A_4}{A_1 A_4^2 A_6 + (1 - A_5 A_6)(A_1 A_3 + k_p^2)} \quad (15)$$

Once$\bar{F}_B^*(k_x,\omega)$has been determined, the stresses are determined with (14) and included in the poroviscoelastic multilayered formulation of the ground (10) to address the solid and relative displacements in the soil. From system (11-13), deflection of the rail, sleepers or ballast can also be deduced.

4. Application to one layer resting on a half-space

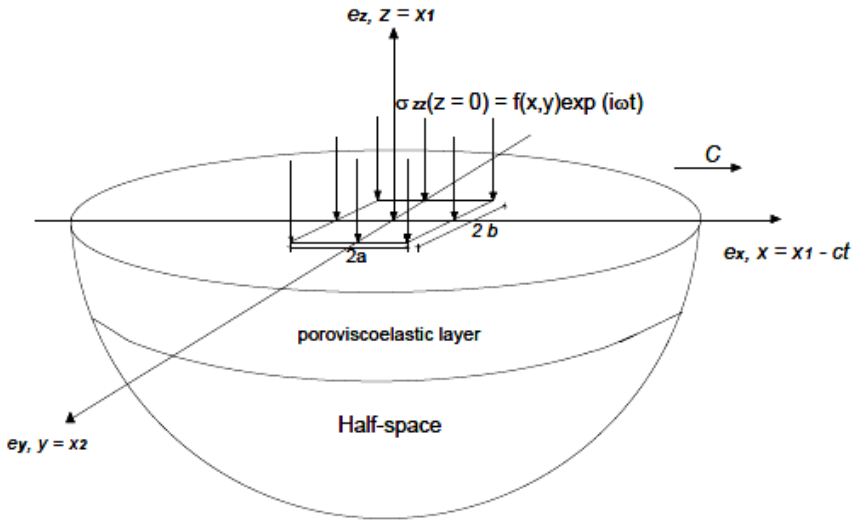

Figure 2: Rectangular moving load acting directly on the soilmedium.

The approach is validated by focusing on the case of a saturated poroviscoelastic layer of 1.0 m depth resting on a rigid half-space with λ_{hs}= 2.33×10^{11}GPa, μ_{hs} = 10^{11}GPa. Parameters of the layer are selected from the bibliography referred to Theodorakopoulos [4]: λ_0= 2.33×10^{8}GPa, μ = 10^{8}GPa, ρ_s = 1816 kg/m^3, ρ_f = 1000 kg/m^3, ϕ = 0.4, β = 1, m = 5.56 GPa and a_1 = 1. Soil dynamic responses deal about a vertical surface solid displacements for a frequency load f = 64 Hz.
First, consider a case of a soil directly subjected to a vertical rectangular load with dimensions 2a×2L_{Bal} moving with a constant velocity c (figure 2). A double Fast Fourier Transform (FFT) algorithm is used to perform the inverse transform with respect to k_x and k_y. To compute the inverse transform accurately with a discrete transform, the integrals must be truncated at sufficiently high values to avoid aliasing, while the mesh of the calculated functions must be fine enough to represent well details of the functions. To satisfy these requirements, we used 2048×2048 points and $|k_x,k_y|< 120$ m^{-1}.
In the case of a soil introducing Sheng's model (see figure 10) an FFT algorithm with 4096×4096 points and a range of $|k_x, k_y| < 40$ m^{-1} is used. The railway is infinite in length and is aligned with respect to the *x* direction. Parameters for the track are those used by Picoux et al. [12]: E = 2.11×10^{11} N.m^{-2}, I = 3055 cm^4, m_R = 60.34 kg.m^{-1}, ms = 191 kg.m^{-1}, kp= 60×10^6 N.m^{-2}, η_p= 0.2, m_B = 1200 kg.m^{-1}, k_B= 3.15×10^8 N.m^2, η_B = 1 and 2L_{Bal} = 1.6 m.

4.1. Contour lines

In this section, contour lines are presented for various values of load velocity, figures 3, 4 and 5. Contours lines are plotted between 10^{-7} m and 10^{-6} m values with isocline step-values 0.5×10^{-7} m.

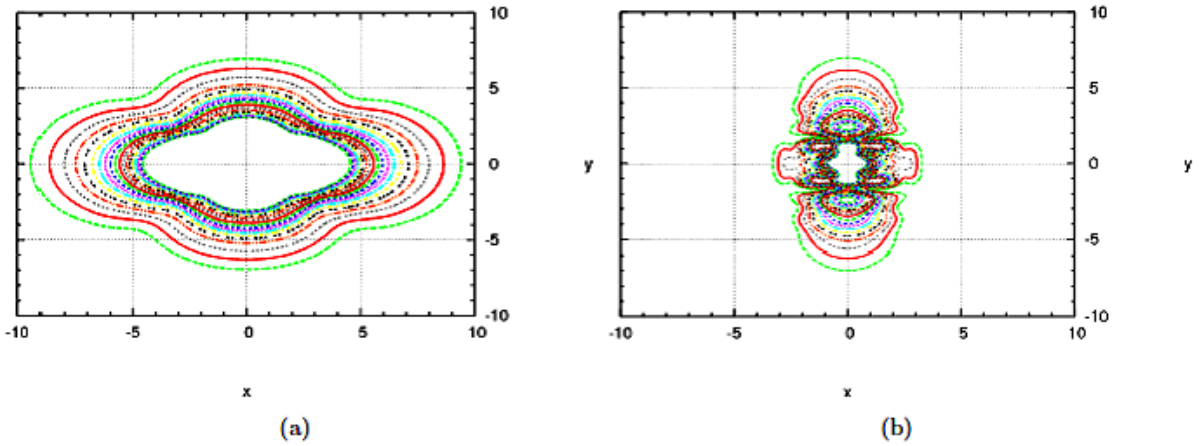

Figure 3: Contour lines of layer displacements, c = 0 m/s: (a) Without track, (b) With track.

In the static case, a more important distribution of displacements along the line x is observed when the load is directly acting on the soil. In the two cases with/without track, displacements are concentrated around the load, Figure 3.

When load is moving, the response begins to spread along the lines*x* and *y*. Nevertheless, the displacements occurring in direction of the motion are still of the same amplitude order, for a low Mach number (i.e. c = 54 $m.s^{-1}$), Figure 4. The displacements are almost equal to zero in frontof the load because the Rayleigh wave which is dominant on the surface and cannot propagate in front of the load since its speed is less than the load speed.

Figure 5 shows a pronounced change in the displacements as the load speed increases andpassesthrough Rayleigh Mach number M_R = 1.5 (c = 163 $m.s^{-1}$). This regime shows importantqualitative behavior: the distribution of displacements spreading behind the load contained within two Mach-lines of higher displacement thus delineating two regions of displacement. The envelope of the Mach-lines through the half-space is called the Mach cone. The angle between the Mach line and the direction of motion is given by: $\phi = \arcsin(1/M_R)$.

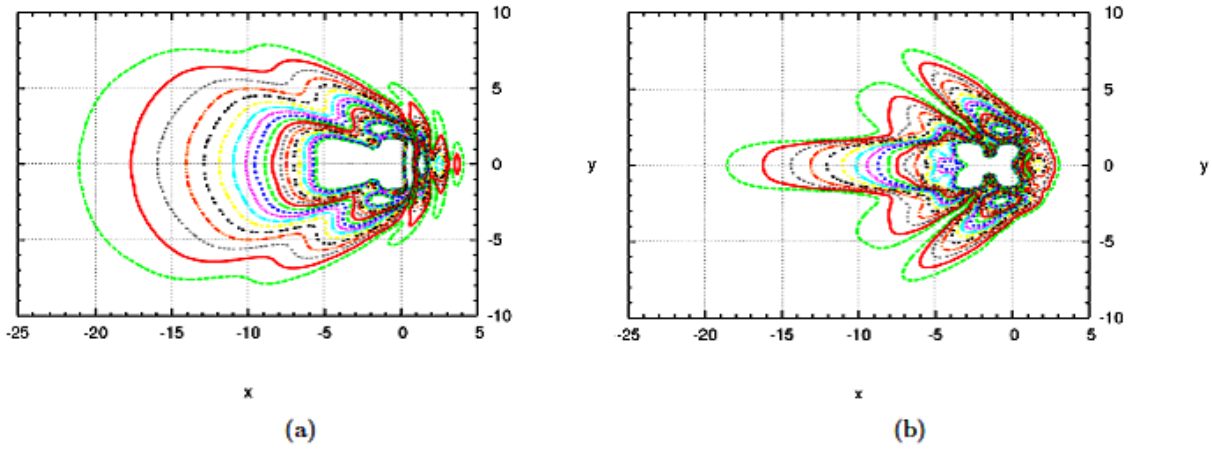

Figure 4: Contour lines of layer displacements, c = 54 m/s: (a) Without track, (b) With track.

When beam is taking into account, the response medium spreads increasingly far behind the excitation but remain concentrated into the Mach cone. Note that the angle closes as we approach the load. For a non-moving load, the presence of beam reduces significantly displacements unlike the case of the moving load and mostly for higher speed load.

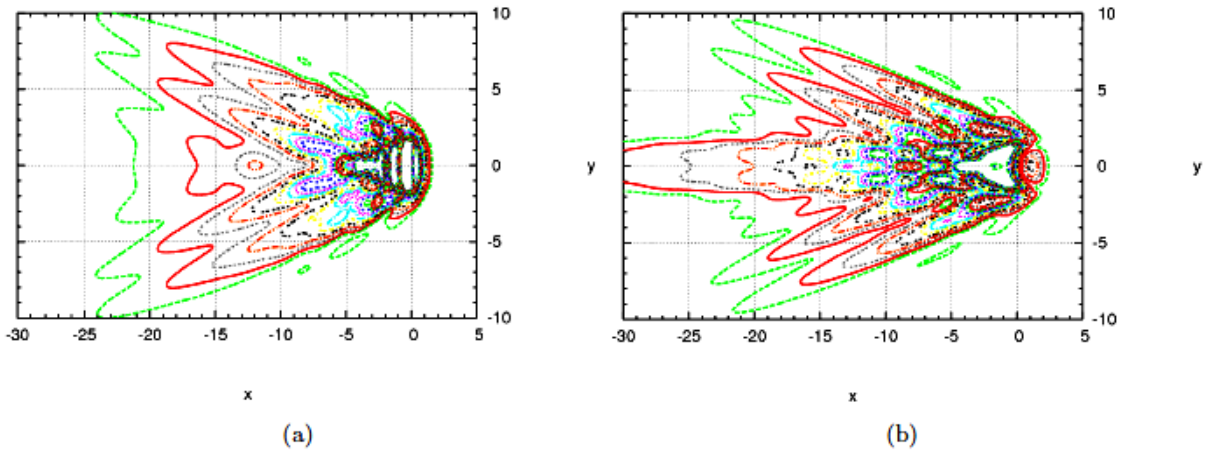

Figure 5: Contour lines of layer displacements, c = 163 m/s: (a) Without track, (b) With track.

4.2. 3D displacements

4.2.1. Static case

Figures 6, 7 and 8 present the evolution of the 3D surface displacements in both with/without track cases, for various Mach numbers.

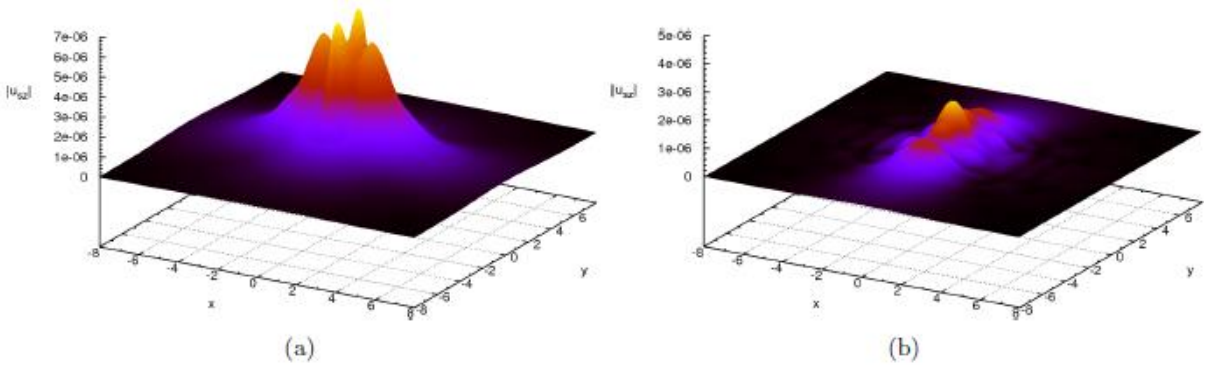

Figure 6: Evolution of layer displacements, MR= 0: (a) Without track, (b) With track.

For the static case (c = 0 $s.m^{-1}$) displacements still remain in the vicinity of the load, this was also observed in the 2D visualization. When the beam is omitted, two peaks appear in the y direction reflecting the distributed displacements in the direction of load, Figure 6 (a). For the other configuration, displacements occur in the x direction. Moreover, the propagating waves changes direction and occurs then, sides of the load when the beam is coupled to the system, Figure 6 (b).

4.2.2. Dynamic case

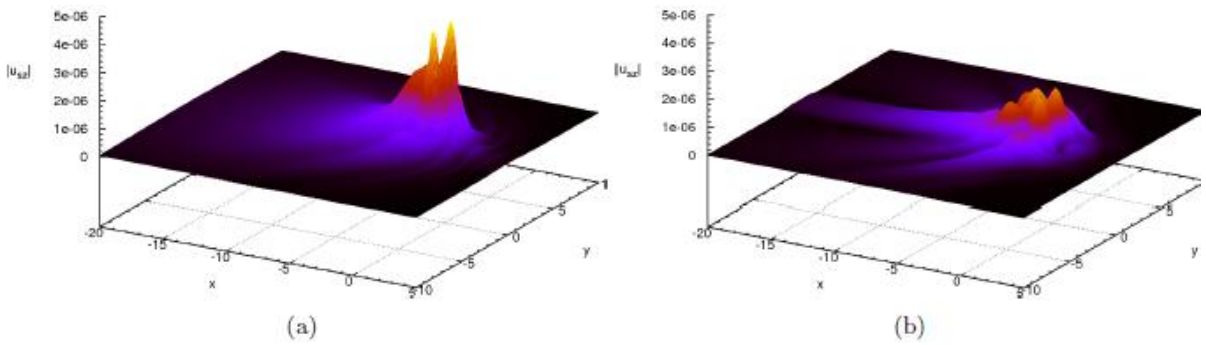

Figure 7: Evolution of layer displacements, MR = 0.5: (a) Without track, (b) With track.

When the load is moving and in absence of beam,a wave propagation occurs and displacements spread further around the load and more particularly behind the load in the sub-Rayleigh regime Figure 7 (a). When the beam is taking into account displacements still spread behind the load and more particularly along the line y, Figure 7 (b).

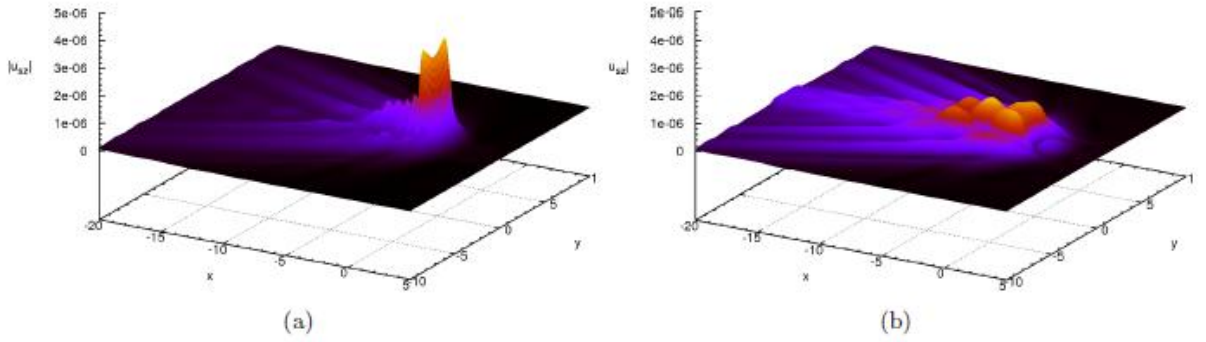

Figure 8: Evolution of layer displacements, MR = 1.5: (a) Without track, (b) With track.

For high speed, displacements amplitude is still maximum along the line y = 0 but displacements are more marked within the Mach cone which is clearly visible for the two configurations, Figures 8 (a) and (b). However, figures show that presence of the track reduces considerably the amplitude of displacements for any load speed. Nevertheless, even if amplitude of soil displacements is lower, the response is as more important far from the loading as speed increases. Therefore, displacements are more important behind the load.

5. Effect of beam on the dynamic response

5.1. Comparison in the spatial domain

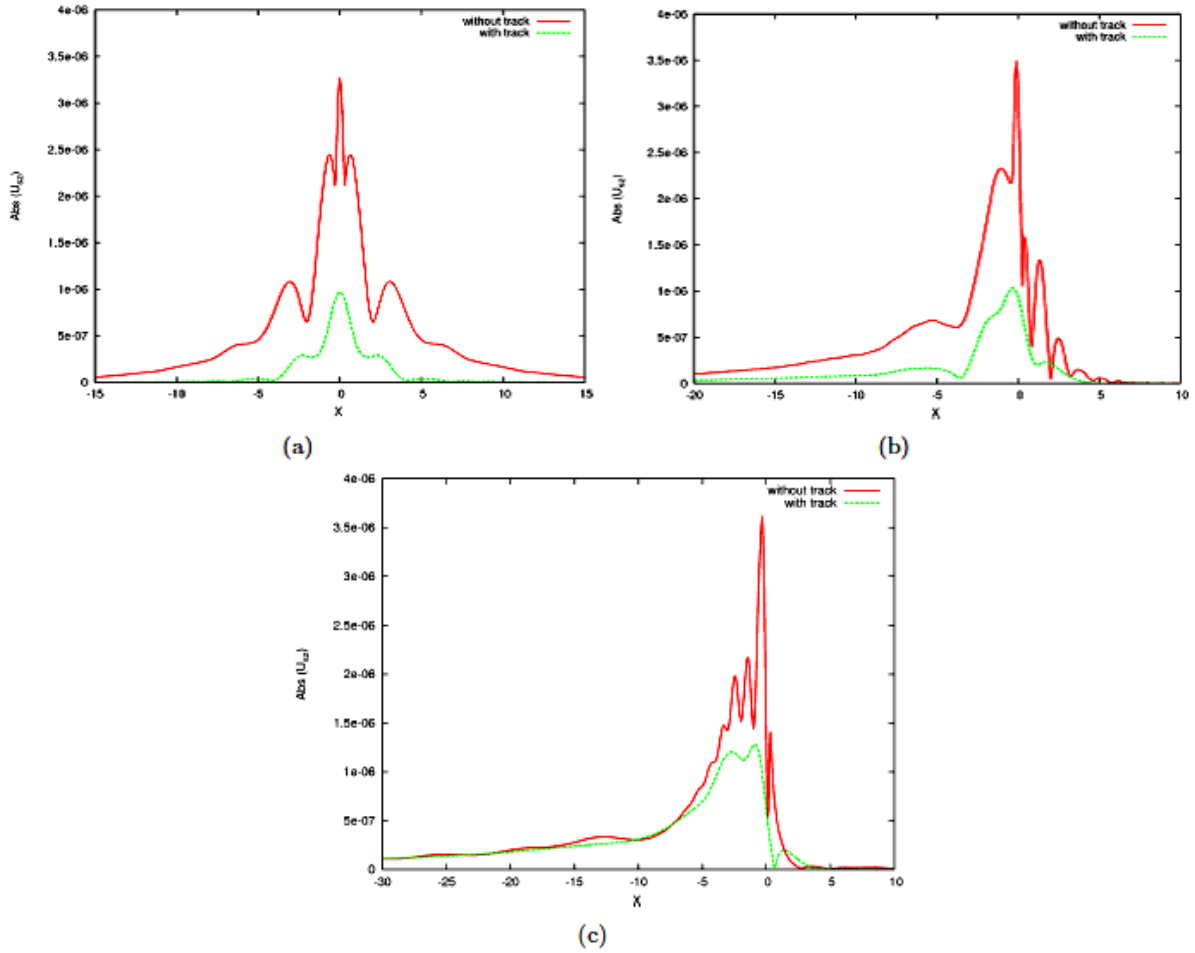

Figure 9: Reduction of soil displacements when introducing the track: (a) $M_R = 0$, (b) $M_R = 0.5$, (c) $M_R = 1.5$

In the spatial domain, displacements are obtained numerically by using a double Fast Fourier Transform (FFT) algorithm to perform the inverse transform with respect to kx and ky. Figure 9 shows a comparison between the case of a load acting directly on the half-space and a case of load acting on the track, for various values of load speed. When the beam is taking into account, displacements are reduced significantly for any value of load speed. Maxima ratios in both cases without/with track is equal to 3.3, 3.4 and 2.8, for $M_R = 0$, $M_R = 0.5$ and $M_R = 1.5$, respectively.

5.2. Comparison in the wavenumber domain

Analysis of displacements in the wavenumber domain allows visualizing the influence of each wave with decoupled manner. The return to the spatial domain is calculated numerically by using the well-known inverse Fast Fourier Transform algorithm (FFT). The real part of displacements is obtained by superposing the contributions of each wave in the spatial domain. Nevertheless, these contributions are mixed, so the contribution of each wave on the dynamic response is not perceptible. Figure 10 illustrates a comparison of a real part of displacements in the wavenumber domain along the line kx = 0, between the cases with/without track.

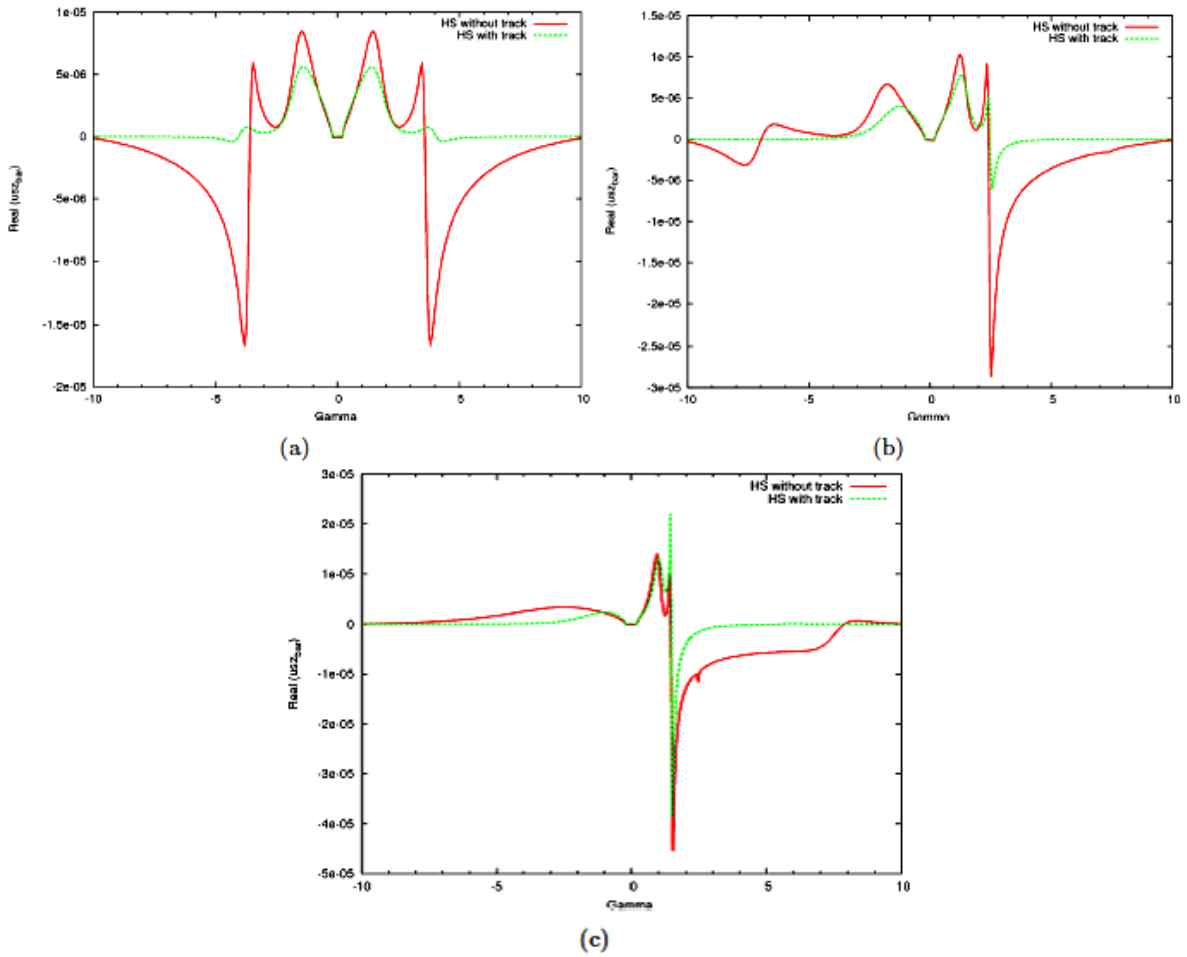

Figure 10: Real part of half-space displacements in the wavenumber domain for $k_x = 0$ line, with/without track : (a) $M_R = 0$, (b) $M_R = 0.5$, (c) $M_R = 1.5$

Figure 10 (a) illustrates a comparison of a real parts of the solid transformed displacements between the cases with/without track, for a non-moving load along the line $k_x = 0$. The figure presents 03 series of peaks: a first series is related to a $\pm k_R$ wavenumbers, another series of peaks is due to a $\pm k_S$ wavenumbers and the last one related to a $\pm k_P$ wavenumbers. The two curves are symmetrical and present two opposite direction of propagation: the positive xdirection (negative wavenumbers) and the negative x direction (positive wavenumbers). The amplitude of peaks relative to the P and S waves are clearly lower than the amplitude of the peaks given by the R one. Contribution of the P wave is similar to the contribution of the Swave (i.e. the real part is positive whereas it is negative for the R wave), but its amplitude is higher. Note that the wavenumbers k_R and k_S are closes to one other. Nevertheless, the amplitude the peak corresponding to the P wave when the beam is taken into account is higher compared to the peak given when the track is omitted and peaks corresponding to the R and S are flattened.

Conclusion

In this paper, a semi-analytical approach to study the wave propagation in a poroviscoelastic layered media has been presented. The approach is based on the theory of Biot, the dynamic response is induced by a vertical harmonic rectangular moving load applied either directly over the soil surface or over the Sheng's track model. This latter takes into account rail, sleepers, pads and ballast, the track

model is coupled to the poroviscoelastic layer resting on a rigid half-space. The implementation of the track allows getting the effect of beam on the dynamic vertical response. Otherwise, numerical results are presented in both the spatial and the wavenumber domains for sub- and super- Rayleigh regimes.

Results deal with the solid vertical displacements on the surface of the soil medium. Results show that displacements are 3 times lower when the track is implemented on the ground. However, the soil dynamic response is reduced for this configuration, in both the static and the dynamic cases and displacements appear in both x and y directions. Otherwise, the amplitude of displacements is more important when the load speed increases, for the two configurations.

References

[1] G. Eason, J. Fulton, I.N. Sneddon,Generation of waves in an infinite elastic solid by variable body forces, Phil Trans Roy Soc A 248, 1956, pp 575-607.
[2] D.V. Jones, D. Le Houédec, A.T. Peplow, M. Petyt,Ground vibration in the vicinity of amoving harmonic rectangular load on a half-space,Eur J Mech, A/Solids 17 (1), 1998, pp 153-66.
[3] F.C.P. De Barros, J.E. Luco, Response of a layered visco-elastic half space to a moving point load,Wave Motion, 19, 1994, pp 189-210.
[4] D.D. Theodorakopoulos,Dynamic analysis of a poroelastic half-plane soil medium under moving loads, Soil DynEarthqEng 23, 2003, pp 521-33.
[5] Cai Y, Sun H, Xu C,Steady state responses of poroelastic half-space soil medium to a moving rectangular load,Int J Solids Struct 44, 2007, pp 7183-96.
[6] Li Shi, A.P.S. Selvadurai. Dynamic response of an infinite beam supported by a saturated poroelastichalfspace and subjected to a concentrated load moving at a constant velocity. Int J Solids Struct, Volumes 88–89, 2016, pp 35-55.
[7] L. Wang, Y. Zhang, S. Tjhen Lie,Detection of damaged supports under railway track based on frequency shift, J Sound Vib, Volume 392, 2017, pp 142-153.
[8] Xu B, Lu JF, Wang JH, Dynamic response of an infinite beam overlying a poroelastic half space to moving loads, J Sound Vib 306, 2007, 91-110.
[9] G. Lefeuve-Mesgouez, A. Mesgouez,Three-dimensional dynamic response of a porous multilayered ground under moving loads of various distributions,AdvEng Software 46, 2012, pp 75-84.
[10] X. Sheng, C.J.C. Jones, M. Petyt,Ground vibration generated by a harmonic load acting on a railway track J Sound vib 225 (1), 1999, pp 3-28.
[11] H. Takemiya, X.C. Bian,Substructure simulation of inhomogeneous track and layered ground dynamic interaction under train passage, J EngMech 131, 2005, pp 699-711.
[12] B. Picoux, D. Le Houédec,Diagnostic and prediction of vibration from railway trains, Soil DynEarthqEng 25, 2005, pp 905-21.
[13] Y. Cai, H. Sun, C. Xu,Three-dimensional simulation of track on poroelastic half-space vibrations due to a moving point load, Soil DynEarthqEng 30, 2010, pp 958-67.
[14]A.V. Vostroukhov, A.V. Metrikine,Periodically supported beam on a visco-elastic layer as a model for dynamic analysis of a high-speed railway track, Int J Sol Struct 40 (21), 2003, pp 5723-52.
[15] A. S.J. Suiker, C. Chang, R. De Borst, C. Esveld,Surface waves in a stratified half space with enhanced continuum properties, part 2: analysis of the wave characteristics in regard to high speed railway tracks,Eur J Mech A/Sol 18, 769-87, 1999.
[16] G. Degrande,G. De Roeck,P. Van Den Broeck, D. Smeulders,Wave propagation in layered dry, saturated and unsaturated poroelastic media,Int J Sol Struct 35 (34-35), 1998, pp 4753-78.